were obtained with AM1 semi-empirical calculations. The positions of the transition states were varied starting from 100 different, randomly chosen starting orientations in a 22.5 Å cube encompassing the antibody variable region. Each simulation involved 150 cycles of simulated annealing. Five flexible dihedral angles of the diene substituent in each transition state were allowed to vary. The energy of interaction was calculated with a potential function composed of van der Waals and Coulombic terms. As a check on this procedure, the ferrocene inhibitor **9** was docked into the antibody; AUTODOCK reproduces the binding position found experimentally to a root mean square (rms) of 0.6 Å.

25. C. Cannizzaro and K. N. Houk, personal communication.
26. E. A. Stura, G. G. Fieser, I. A. Wilson, *Immunomethods* **3**, 164 (1993).
27. The x-ray crystallographic programs and methods used were the following. (i) DENZO and SCALEPACK: Z. Otwinowski, in *Data Collection and Processing*, L. Sawyer, N. Isaacs, S. Bailey, Eds. (SERC Daresbury Laboratory, Warrington, UK, 1993), p. 56; (ii) MERLOT: P. M. D. Fitzgerald, *J. Appl. Crystallogr.* **21**, 273 (1988); (iii) AMORE: J. Navaza, *Acta Crystallogr.* **A50**, 157 (1994); (iv) O: T. A. Jones, J.-Y. Zou, S. W. Cowan, M. Kjeldgaard, *ibid.* **A47**, 110 (1991); (v) X-PLOR: A. T. Brünger, J. Kuriyan, M. Karplus, *Science* **235**, 458 (1987); A. T. Brünger, *X-PLOR, Version 3.1: A System for X-ray and NMR* (Yale Univ. Press, New Haven, CT, 1992); (vi) SHELXL,SHELXS,SHELXPRO: G. M. Sheldrick, SHELXL-96, Program for crystal structure refinement, University of Göttingen (1996); (vii) sigma-A: R. J. Read, *Acta Crystallogr.* **A42**, 140 (1986).
28. A. Heine, E. A. Stura, K. D. Janda, I. A. Wilson, unpublished data.
29. R. L. Stanfield, T. M. Fieser, R. A. Lerner, I. A. Wilson, *Science* **248**, 712 (1990).
30. J. H. Arevalo, E. A. Stura, M. J. Taussig, I. A. Wilson, *J. Mol. Biol.* **231**, 103 (1993).
31. The graphics programs used were the following. (i) AVS: C. Upson *et al.*, *IEEE Comput. Graph. Appl.* **9**, 30 (1989); (ii) XP: SHELXTL 5.03, Siemens Industrial Automation, Inc., Madison, WI, 1990–1995; MOLMOL: R. Koradj, M. Billeter, K. Wüthrich, *J. Mol. Graph.* **14**, 51 (1996).
32. G. D. Purvis and C. Culberson, *J. Mol. Graph.* **4** (1986).
33. We thank M. Pique for production of figures, the Stanford Synchrotron Radiation Laboratory for data collection time, and the staff of beamline 7-1 for their assistance; G. Fieser and R. Stefanko for technical assistance, C.-H. Lo for Fab sequence determination, R. Stanfield and K. Gruber for discussions and comments, K. Renner for computational assistance, D. McRee for map generation in XFIT, R. Lerner for support and encouragement, and R. Chadha for data collection of **9**. Supported by NIH grants PO1 CA27489 (I.A.W. and K.D.J.) and GM-43858 (K.D.J.), NSF grant CHE9120588 (K.N.H.), and a fellowship by TEKES, Technology Development Centre, The Finnish Centre for International Mobility and Exchange Programmes, Helsinki, Finland (J.Y-K). This is publication 11111-MB from The Scripps Research Institute. The coordinates have been deposited in the Brookhaven databank with access code 1a3l and are available immediately from wilson@scripps.edu or aheine@scripps.edu.

18 September 1997; accepted 30 January 1998

RNA Folding at Millisecond Intervals by Synchrotron Hydroxyl Radical Footprinting

Bianca Sclavi, Michael Sullivan, Mark R. Chance,* Michael Brenowitz,* Sarah A. Woodson*

Radiolysis of water with a synchrotron x-ray beam permits the hydroxyl radical–accessible surface of an RNA to be mapped with nucleotide resolution in 10 milliseconds. Application of this method to folding of the *Tetrahymena* ribozyme revealed that the most stable domain of the tertiary structure, P4-P6, formed cooperatively within 3 seconds. Exterior helices became protected from hydroxyl radicals in 10 seconds, whereas the catalytic center required minutes to be completely folded. The results show that rapid collapse to a partially disordered state is followed by a slow search for the active structure.

The speed of chemical reactions carried out by ribozymes is often limited by conformational changes in the RNA (*1*). As a result, the process by which RNA molecules fold into their native conformation has received much attention. Early investigations into the folding of tRNA established approximate time scales for the formation of RNA secondary (10^{-4} to 10^{-5} s) and tertiary interactions (10^{-2} to 10^{-1} s), with the reorganization of incorrect secondary structures occurring more slowly (0.1 to 1 s) (*2*). Recent work has shown that folding of large RNAs is more complex (*3*), involving multiple pathways (*4*). Individual domains of an RNA may form at rates that differ by orders of magnitude, with some transitions requiring minutes to reach completion (*3–7*). Identification of the paths by which large RNAs fold has been hampered by the lack of experimental methods capable of probing RNA conformation with nucleotide resolution at subsecond time scales (*8*). Here, we describe direct measurement of the complete folding pathway of the *Tetrahymena* ribozyme by hydroxyl radical footprinting using a synchrotron x-ray beam.

Hydroxyl radical ribose oxidation and resulting strand cleavage are correlated with the solvent accessibility of the RNA backbone (*9*, *10*) and are insensitive to base sequence and secondary structure (*11*). Generation of hydroxyl radicals by the radiolysis of water yields cleavage products that are comparable with Fe(II)-EDTA–dependent reactions (*7*, *12*). The high flux provided by white-light x-ray beams at the National Synchrotron Light Source (NSLS) permits footprinting of the ribozyme to be accomplished with millisecond time resolution (*7*).

The ribozyme derived from the *Tetrahymena* group I intron (Fig. 1A) folds into a well-defined tertiary structure in the presence of Mg^{2+}, and Mg^{2+} is required for catalytic activity (*1*). The ribozyme contains at least three domains of tertiary structure (*13*) that, when separated, can reassociate to form the active ribozyme (*14*). The domain containing paired regions P4-P6 (Fig. 1A) folds independently (*10*, *15*), and formation of P4-P6 has been proposed to be the first step in the folding pathway of the ribozyme (*3*, *16*). In earlier experiments in which RNA was manually mixed with Mg^{2+} before exposure to the x-ray beam, we showed that the tertiary structure of the P4-P6 domain is formed within 30 s, the initial time of the assay (*7*).

To resolve early steps in the ribozyme folding pathway, we installed a stopped-flow apparatus with an x-ray exposure chamber on NSLS beamline X-9A (*17*). The flux of X-9A absorbed by the sample was sufficient to cleave 20% of the RNA molecules with exposures as short as 10 ms (*18*). Folding reactions were begun by mixing RNA with buffer containing Mg^{2+}, to a final concentration of 10 mM (*19*). Samples were irradiated at a series of times after mixing, and the hydroxyl radical cleavage products were separated by gel electrophoresis (*19*). The ribozyme was fully active after passage through the stopped-flow apparatus (*20*), verifying that the RNA had folded correctly under these experimental conditions.

We determined the folding kinetics of the ribozyme by quantitating the changes in solvent accessibility of individual sites as a function of time (Fig. 2) (*7*, *21*). After the addition of Mg^{2+}, specific nucleotides within the P4-P6 domain became protected from cleavage within 100 ms (*22*), and the extent of protection reached a plateau within several seconds (Fig. 2). Comparison of this plateau with control reactions,

B. Sclavi, M. Sullivan, M. R. Chance, Department of Physiology and Biophysics, Center for Synchrotron Biosciences, Albert Einstein College of Medicine of Yeshiva University, 1300 Morris Park Avenue, Bronx, NY 10461, USA.
M. Brenowitz, Department of Biochemistry, Center for Synchrotron Biosciences, Albert Einstein College of Medicine of Yeshiva University, 1300 Morris Park Avenue, Bronx, NY 10461, USA.
S. A. Woodson, Department of Chemistry and Biochemistry, University of Maryland, College Park, MD 20742–2021, USA.
*To whom correspondence should be addressed.

in which the ribozyme was preequilibrated in Mg^{2+} before the start of the experiment, demonstrates that folding of P4-P6 was complete within this time (Fig. 2, triangles).

The rapidly protected sites correspond to nucleotides that were excluded from solvent by folding of the P4-P6 domain upon itself (Fig. 1, A and B). These rapidly protected sites include nucleotides in P5 and P5a, an A-rich bulge, and a GAAA tetraloop that are involved in interactions that stabilize the tertiary structure of the domain (*15*, *23*). Rate constants determined for each of these regions (Fig. 1A, orange) were the same within experimental error. Thus, the tertiary interactions within the P4-P6 domain were established in a concerted manner at a rate of about 1 s^{-1} at 42°C.

A subset of nucleotides in P5c (Fig. 1A, green) was protected about twice as rapidly as other regions in the P4-P6 domain. Protection of riboses in P5c results from local interactions that bury the P5c backbone (*15*). P5a-P5c constitutes a Mg^{2+}-rich subdomain that folds independently of interactions with P4 and P6 (*15*, *24*). Although the differences in the rate constants determined for these nucleotides are at the limit of the precision of the data, these results suggest that formation of a metal ion "core" in P5a-P5c (*24*) is one of the earliest folding transitions of the ribozyme. This region could serve as a nucleation site for additional tertiary structure.

Several groups of nucleotides are protected from hydroxyl radicals by tertiary contacts that are present in the ribozyme but not in the isolated P4-P6 domain (*15*). Residues in P5 (118 to 121) and joining region J5/4 (204 to 208) are protected by folding of P9.1 and P9.2 (*25*). The 5′ and 3′ ends of the P4-P6 domain are part of a triple helix that mediates interactions with double helices P3 and P7 (*14*). Both groups of nucleotides (Fig. 1A, pink) became protected more slowly ($k \sim 0.3\ s^{-1}$) than the interior of P4-P6. Thus, tertiary contacts with the P3-P9 domain (P3, P7, P8, and P9) formed after the P4-P6 domain was folded. This is consistent with the observation that tertiary interactions with P4-P6 stabilize the folded structure of P3-P9 (*13*, *25*, *26*).

In agreement with this conclusion, nucleotides in P2, P2.1, and P9.1 were protected from hydroxyl radical cleavage at similar rates (k = 0.2 to 0.4 s^{-1}) (Fig. 1A, pink). These helices bridge the two central domains of the ribozyme, stabilizing the catalytic center by base pairing between the loops L2 and L5c and L2.1 and L9.1 (*27*). P2-P2.1 and P9.1-P9.2 are proposed to wrap around the exterior of the folded ribozyme, and protection from hydroxyl radical cleavage results from contacts with the folded P4-P6 and P3-P9 domains (*26*, *27*). Thus, much of the tertiary structure is formed in about 10 s.

In contrast, P3, P7, and P9 required minutes (k = 0.02 to 0.06 s^{-1}) to become fully protected from hydroxyl radical cleavage (Fig. 1A; yellow). This result is consistent with our earlier results (*7*) and with oligonucleotide hybridization and chemical modification data showing that P3 and P7 are the last stems to form completely (*3*, *5*, *7*). Protection of nucleotides in P6 (220 to 222) is attributed to close packing with the stacked P3 and P8 helices (*27*), and it appeared at a similar rate (k = 0.03 s^{-1}) (Fig. 1A). Thus, the P3-P9 sequences remain disordered until late in the folding process. Solvent accessibility of P3-P9 could result from either a highly extended conformation or from a mixture of conformations with nonoverlapping footprints that are in slow exchange.

The ability to probe solvent-accessible regions of an RNA backbone within the first tens of milliseconds of a reaction provides a visualization of early steps in the folding pathway of the *Tetrahymena* ribozyme. An assumption of the model depicted in Fig. 3 is that much of the secondary structure is formed under the initial conditions of our assay (no Mg^{2+} and 42°C). After the addition of Mg^{2+}, the earliest evidence of tertiary structure appeared within the P5a-P5c subdomain. Subsequent collapse of the P4-P6 domain

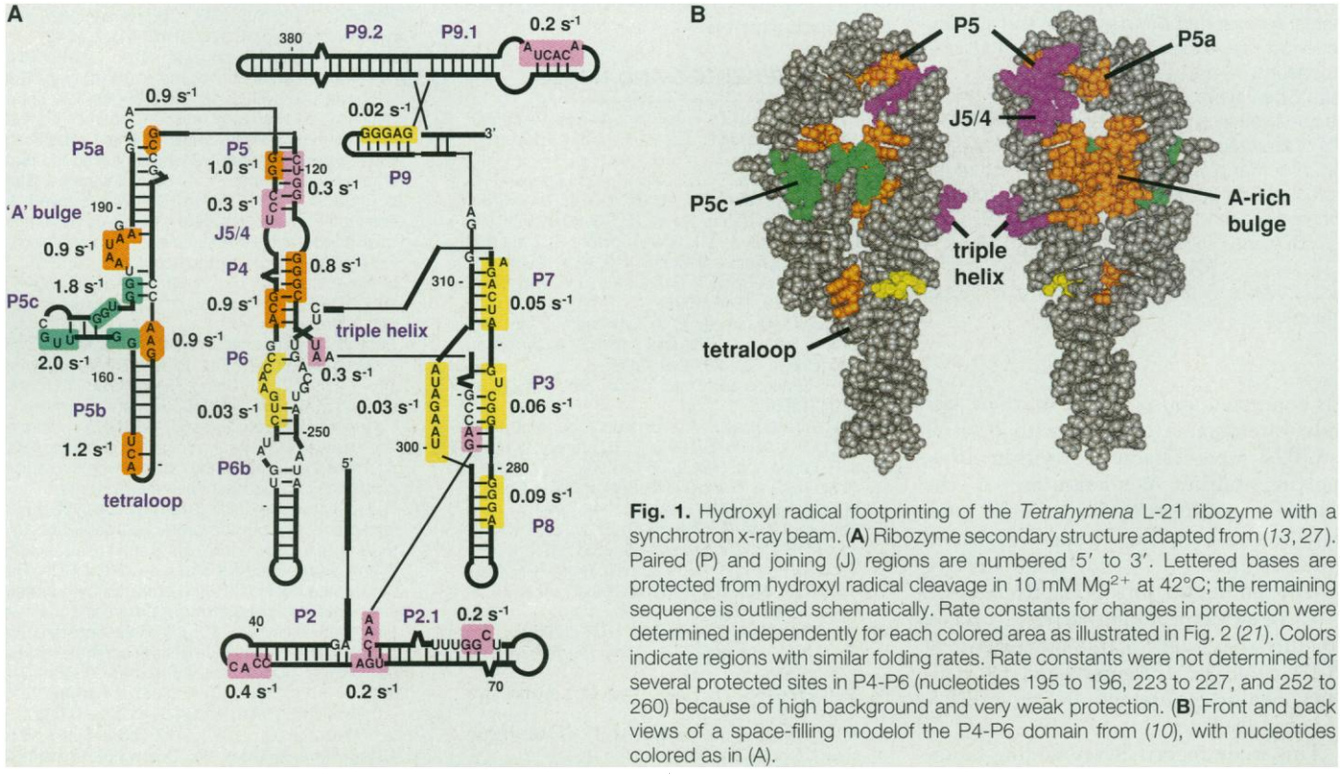

Fig. 1. Hydroxyl radical footprinting of the *Tetrahymena* L-21 ribozyme with a synchrotron x-ray beam. (**A**) Ribozyme secondary structure adapted from (*13*, *27*). Paired (P) and joining (J) regions are numbered 5′ to 3′. Lettered bases are protected from hydroxyl radical cleavage in 10 mM Mg^{2+} at 42°C; the remaining sequence is outlined schematically. Rate constants for changes in protection were determined independently for each colored area as illustrated in Fig. 2 (*21*). Colors indicate regions with similar folding rates. Rate constants were not determined for several protected sites in P4-P6 (nucleotides 195 to 196, 223 to 227, and 252 to 260) because of high background and very weak protection. (**B**) Front and back views of a space-filling modelof the P4-P6 domain from (*10*), with nucleotides colored as in (A).

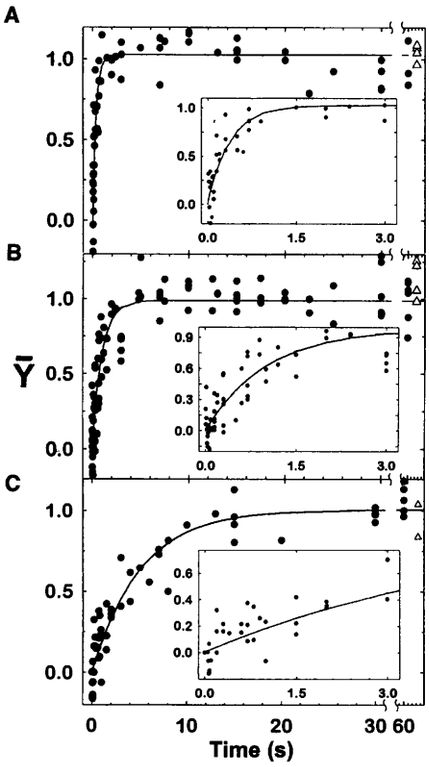

Fig. 2. Time dependence of hydroxyl radical protection. Fractional saturation of individual protected sites, $\bar{Y}$, was determined from fits to the coupled equations $p = p_{lower} + (p_{upper} - p_{lower})\,\bar{Y}$ and $\bar{Y} = 1 - e^{-kt}$, where p is the apparent saturation, p_{lower} and p_{upper} are the lower and upper limits of the transition curve, respectively, k is the first-order rate constant, and t is time (in seconds). Data from three to six independent experiments were plotted simultaneously and fit to the first-order rate expression (solid line). Additional exponential terms were not supported by the data. Open symbols represent controls in which the ribozyme was preequilibrated with Mg^{2+}. Details of the data analysis are described elsewhere (*29*). A similar plot was produced for each of the protected sites shown in Fig. 1A. (**A**) Protection of P5c, nucleotides 174 to 176; k = 2.7 (−1.3, +1.8) s^{-1}. (**B**) A-rich bulge, nucleotides 183 to 189; k = 0.9 (±0.3) s^{-1}. (**C**) P2, nucleotides 57 to 59; k = 0.20 (±0.05) s^{-1}. (**Insets**) Expansion of first 3 s of time axis.

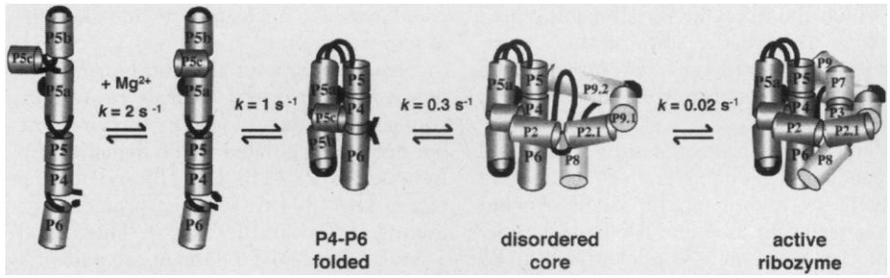

Fig. 3. A model for the early steps of the Mg^{2+}-dependent folding of the *Tetrahymena* ribozyme. Residues in P5c become protected most rapidly, about twofold faster than nucleotides in the interior of the P4-P6 domain. Nucleotides that are excluded from solvent by interactions with P2-P2.1 and the P3-P9 domain are protected more slowly. Ordering of the catalytic core occurs over several minutes (*3*, *5*, *7*) and may involve reorganization of alternative conformations after collapse to a partially disordered intermediate state. For simplicity, folding is depicted as a linear sequence of events, although there are likely to be multiple folding pathways with different intermediates (*4*). Some molecules in the population may reach the native state rapidly, whereas others fold slowly because of the presence of kinetic traps.

was concerted and occurred in a few seconds. Interdomain contacts with P2-P2.1 and P9.1 were established within 10 s, implying further condensation of the RNA. Organization of the catalytic core, including formation of P3 and P7, is about tenfold slower (*3*, *7*) and could involve either local fluctuations of the RNA chain or rearrangement of alternative secondary structures (*4*, *5*, *28*). Large movements of P3-P9 could be accommodated by transient opening of interactions between P2-P2.1 and P9.1.

This study reports RNA folding kinetics in which condensation of tertiary structure occurred at rates similar to that of in vivo self-splicing (*29*). Folding of the P4-P6 domain of the *Tetrahymena* ribozyme was only tenfold slower (1 s^{-1}) than formation of tertiary interactions in tRNA (100 ms) (*2*). Folding of P4-P6 and interactions with P2 rapidly reduce the number of available conformations. The catalytic center, however, remains disordered until late in the folding process; final steps occur after the RNA has become compact. Because formation of the native structure requires condensation of the RNA and coordination of multiple Mg^{2+} ions (*15*, *24*), the fast folding events may be sensitive to solvation and divalent ion concentration.

REFERENCES AND NOTES

1. T. R. Cech and D. Herschlag, *Nucleic Acids Mol. Biol.* **10**, 1 (1996); L. Jaeger, F. Michel, E. Westhof, *ibid.*, p. 34.
2. D. M. Crothers, P. E. Cole, C. W. Hilbers, R. G. Shulman, *J. Mol. Biol.* **87**, 63 (1974); reviewed in D. E. Draper, *Nature Struct. Biol.* **3**, 397 (1996).
3. P. P. Zarrinkar and J. R. Williamson, *Science* **265**, 918 (1994); *Nature Struct. Biol.* **3**, 432 (1996); D. K. Treiber, M. S. Rook, P. P. Zarrinkar, J. R. Williamson, *Science* **279**, 1943 (1998).
4. J. Pan, D. Thirumalai, S. A. Woodson, *J. Mol. Biol.* **273**, 7 (1997); D. Thirumalai and S. A. Woodson, *Acc. Chem. Res.* **29**, 433 (1996).
5. A. R. Banerjee and D. H. Turner, *Biochemistry* **34**, 6504 (1995).
6. V. L. Emerick and S. A. Woodson, *Proc. Natl. Acad. Sci. U.S.A.* **91**, 9675 (1994); P. P. Zarrinkar, J. Wang, J. R. Williamson, *RNA* **2**, 564 (1996).
7. B. Sclavi, S. A. Woodson, M. Sullivan, M. R. Chance, M. Brenowitz, *J. Mol. Biol.* **266**, 144 (1997).
8. Reviewed in M. R. Chance, B. Sclavi, S. A. Woodson, M. Brenowitz, *Structure* **5**, 865 (1997).
9. T. D. Tullius and B. A. Dombroski, *Proc. Natl. Acad. Sci. U.S.A.* **83**, 5469 (1986); J. A. Latham and T. R. Cech, *Science* **245**, 276 (1989).
10. J. H. Cate *et al.*, *Science* **273**, 1678 (1996).
11. D. W. Celander and T. R. Cech, *Biochemistry* **29**, 1355 (1990).
12. M. A. Price and T. D. Tullius, *Methods Enzymol.* **212**, 194 (1992).
13. T. R. Cech, S. Damberger, R. R. Gutell, *Nature Struct. Biol.* **1**, 273 (1994).
14. J. A. Doudna and T. R. Cech, *RNA* **1**, 31 (1995).
15. F. L. Murphy and T. R. Cech, *Biochemistry* **32**, 5291 (1993).
16. D. W. Celander and T. R. Cech, *Science* **251**, 401 (1991); W. D. Downs and T. R. Cech, *RNA* **2**, 718 (1996).
17. A three-syringe quench-flow device (Kin-Tek, State College, PA) was modified to incorporate an x-ray exposure chamber. Details of the design, installation, and beamline configuration will appear elsewhere (*30*). The configuration of beamline X-9A allows for footprinting to be conducted with substantially shorter x-ray exposures than previously reported (*7*).
18. Contributions from direct absorption of x-rays by the RNA were negligible, because of the 10^9-fold greater concentration of water molecules.
19. 5′ ^{32}P-labeled 385-nucleotide L-21 Sca I ribozyme was prepared as previously described [A. J. Zaug, C. A. Grosshans, T. R. Cech, *Biochemistry* **27**, 8924 (1988)]. RNA was annealed by slow cooling from 90° to 42°C in 10 mM Na-cacodylate and 0.1 mM EDTA (pH 7.5) (CE). Control samples were preequilibrated in CE plus 10 mM $MgCl_2$ at 42°C for 40 min. To begin folding, we mixed 12 μl of RNA (10 nM) with an equal volume of 20 mM $MgCl_2$ in CE using two syringes of the stopped-flow apparatus (*17*) and sampled reactions at times from 20 ms to 8 min. Samples within a single experiment were exposed to the X-9A beam for an identical time. Exposure times (10 to 50 ms) were adjusted so that 10 to 30% of the RNA was cleaved, to ensure that molecules were cleaved no more than once on average. RNA samples (70 μl final volume) were precipitated after the addition of 15 μl of 1.5 M Na-acetate (pH 5), carrier tRNA (0.25 mg/ml), and 300 μl of ethanol and analyzed by denaturing gel electrophoresis (*7*).
20. Catalytic activity after 1 to 15 min of folding was assayed by expelling samples (15 nM ribozyme) into a solution containing 75 nM $GGCCCUCUA_5$ and 0.5 mM guanosine triphosphate and measuring the initial rate of cleavage of the RNA substrate. The increase in the fraction of active ribozyme (0.02 s^{-1}) was the same as the rate of hydroxyl radical protection of residues in the catalytic center.
21. Rate constants for folding transitions can be determined directly from the protection data, because the time of exposure to x-rays is short relative to the changes in the tertiary structure of the RNA. Reported rate constants were obtained by nonlinear least squares analysis of the progress curves as described elsewhere (*7*, *30*). Rate constants (in s^{-1}; with 65% confidence limits in parentheses) are as follows: nucleotides 45 to 48, 0.42 (−0.1, +0.15); 57 to 59, 0.20 (±0.05); 81 to 83, 0.15 (−0.05, +0.06); 93 to 97, 0.16 (−0.02, +0.04); 105 to 106, 0.3 (±0.1); 109 to 112, 0.8 (±0.4); 118 to 121, 0.3 (±0.2); 125 to 126, 0.9 (±0.5); 139 to 140,

0.9 (±0.4); 153 to 155, 1.3 (±0.5); 163 to 164, 1.6 (−0.7, +0.9); 167 to 170, 2.0 (−0.6, +0.8); 174 to 175, 2.7 (−1.3, +1.8); 180 to 181, 1.8 (±0.6); 183 to 189, 0.9 (±0.3); 200 to 203, 1.0 (−0.4, +0.6); 204 to 208, 0.3 (±0.1); 212 to 215, 0.9 (±0.5); 220 to 222, 0.03; 263 to 268, 0.05; 272 to 276, 0.06; 280 to 283, 0.1 (−0.2, +0.3); 300 to 306, 0.03; 327 to 331, 0.02 (−0.006, +0.02); and 342 to 347, 0.3 (−0.1, +0.2).

22. A sequence-independent decrease in the extent of cleavage after the addition of Mg^{2+} was observed within the dead time of the experiment (20 ms). Because a similar result was obtained with 0.5 to 1.0 M KCl, we attribute this decrease to either a general electrostatic effect on ribose oxidation or a decrease in the steady-state concentration of hydroxyl radical, rather than to any specific folding transition in the RNA. However, it is possible that monovalent cations induce a conformational change within the first 20 ms (*28*).
23. F. L. Murphy and T. R. Cech, *J. Mol. Biol.* **236**, 49 (1994).
24. J. H. Cate, R. L. Hanna, J. A. Doudna, *Nature Struct. Biol.* **4**, 553 (1997).
25. B. Laggerbauer, F. L. Murphy, T. R. Cech, *EMBO J.* **13**, 2699 (1994).
26. E. A. Doherty and J. A. Doudna, *Biochemistry* **36**, 3159 (1997).
27. V. Lehnert, L. Jaeger, F. Michel, E. Westhof, *Chem. Biol.* **3**, 993 (1996).
28. P. E. Cole, S. K. Yang, D. M. Crothers, *Biochemistry* **11**, 4358 (1972).
29. S. L. Brehm and T. R. Cech, *ibid.* **22**, 2390 (1983).
30. B. Sclavi, S. A. Woodson, M. Sullivan, M. R. Chance, M. Brenowitz, *Methods Enzymol.*, in press.
31. Supported by grants from NIH (GM39929, GM51506, and GM52348), the Molecular Biophysics Training Program (GM08572), NSF (MCB-9410748 and MCB-9601148), and the Hirschl Weill-Caulier Trust. S.W. acknowledges the Pew Scholars Program and the Henry and Camille Dreyfus Foundation. The construction and operation of beamline X-9A are supported by the National Center for Research Resources, Biomedical Technology Program (P41-RR01633). The NSLS is supported by the Department of Energy, Division of Materials Sciences. The data in this paper are from a thesis to be submitted by B.S. in partial fulfillment of the requirements for the degree of Doctor of Philosophy in the Sue Golding Graduate Division of Medical Sciences, Albert Einstein College of Medicine.

20 August 1997; accepted 14 January 1998

Kinetic Intermediates Trapped by Native Interactions in RNA Folding

Daniel K. Treiber, Martha S. Rook, Patrick P. Zarrinkar,* James R. Williamson†

In the magnesium ion–dependent folding of the *Tetrahymena* ribozyme, a kinetic intermediate accumulates in which the P4-P6 domain is formed, but the P3-P7 domain is not. The kinetic barriers to P3-P7 formation were investigated with the use of in vitro selection to identify mutant RNA molecules in which the folding rate of the P3-P7 domain was increased. The critical mutations disrupt native tertiary interactions within the P4-P6 domain and increase the rate of P3-P7 formation by destabilizing a kinetically trapped intermediate. Hence, kinetic traps stabilized by native interactions, and not simply by mispaired nonnative structures, can present a substantial barrier to RNA folding.

RNA forms complex structures that are able to perform a variety of functions ranging from ligand binding to catalysis. However, the mechanism by which an RNA molecule folds into a unique three-dimensional structure remains poorly understood. To study the Mg^{2+}-dependent kinetic folding pathways of large, highly structured RNA molecules such as the *Tetrahymena* ribozyme and ribonuclease (RNase) P, we have previously developed a kinetic oligonucleotide hybridization assay (*1*, *2*). This assay exploits the selective accessibility of unfolded RNAs to sequence-specific oligodeoxynucleotide probes, the binding of which confers sensitivity to cleavage by RNase H. Folding is initiated by the addition of Mg^{2+}, and the fraction of unfolded RNA at various times is scored in a cleavage reaction containing DNA probes and RNase H. On addition of Mg^{2+} to the *Tetrahymena* ribozyme, the two structural domains that constitute the catalytic core—P4-P6 [base-paired (P) regions 4 to 6, positions 104 to 261] and P3-P7 (P3, P7, and P8)—form sequentially as kinetic folding units (*1*, *3*). Formation of P4-P6 is rapid (60 min^{-1}) (*4*), whereas P3-P7 forms slowly, on the minute time scale (*1*). This order of kinetic folding events is supported by chemical modification (*5*), ultraviolet cross-linking (*6*), and x-ray footprint (*4*) analysis. In the proposed folding pathway (*1*, *3*), an intermediate (I_2) accumulates in which only P4-P6 is folded, and the rate-limiting step for P3-P7 formation is the unimolecular rearrangement of I_2 to intermediate I_3. Slow unimolecular folding steps have also been identified for the group I intron b15 (*7*) and RNase P (*2*), and they may be a general feature in the folding of large RNAs.

Mutations that increase the rate of folding of proteins have provided insight into the mechanism of slow folding steps (*8*). We developed an in vitro selection scheme to identify mutant *Tetrahymena* ribozymes in which the slow P3-P7 folding step ($I_2 \rightarrow I_3$) is accelerated (*9*). Ribozymes that fold rapidly after Mg^{2+} addition were selected from a pool of RNAs containing an average of four mutations per molecule. Slow-folding RNAs were selectively depleted from the pool by kinetic oligonucleotide hybridization with probes targeting P3 and P7. A step was included in each cycle of selection to ensure that fast folding mutants formed an intact catalytic core (*9*). After nine rounds, the folding rate of the pool (G_9) had increased by a factor of 4 relative to that of the initial pool (G_0) and by a factor of 2 relative to that of the wild type (Fig. 1). Twenty-four individual molecules were cloned from the G_9 pool, and the folding rate of the P3-P7 domain for five of these clones was at least three to five times that of the wild type at 37°C (Fig. 1 and Table 1) (*10*, *11*).

Because each fast folding clone contained at least three mutations, individual point mutants were constructed. For the four clones analyzed, a single mutation was sufficient to reproduce the fast folding phenotype (Table 1). The A183U (A at posi-

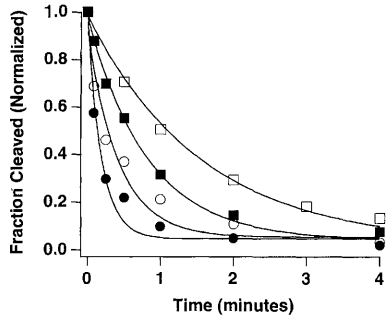

Fig. 1. Isolation of fast folding RNAs after nine rounds of in vitro selection. The kinetics of P3-P7 formation for ribozyme generations G_0 to G_9 and cloned individual molecules from G_9 were probed by kinetic oligonucleotide hybridization. Initiation of folding and the quench reaction were as described (*9*). The fraction cleaved at each folding time was determined by denaturing PAGE and Phosphorimager analysis (Molecular Dynamics). The apparent folding rate constant (k_{fold}) was calculated by fitting curves to a single exponential (*10*). Data were normalized to allow direct comparison. RNAs and k_{fold} values: □, G_0 pool (0.63 min^{-1}), ■, wild type (1.2 min^{-1}), ○, G_9 pool (2.33 min^{-1}), and ●, clone G_9-10 (5.0 min^{-1}).

D. K. Treiber and J. R. Williamson, Department of Molecular Biology, MB33, Scripps Research Institute, 10550 North Torrey Pines Road, La Jolla, CA 92037, USA.
M. S. Rook and P. P. Zarrinkar, Department of Chemistry, Massachusetts Institute of Technology, Cambridge, MA 02139, USA.
*Present address: Center for Cellular and Genetic Therapies, Department of Surgery, Duke University Medical Center, Durham, NC 27710, USA.
†To whom correspondence should be addressed.